Plasmonic Nanostructures II

Propagation of SPPs

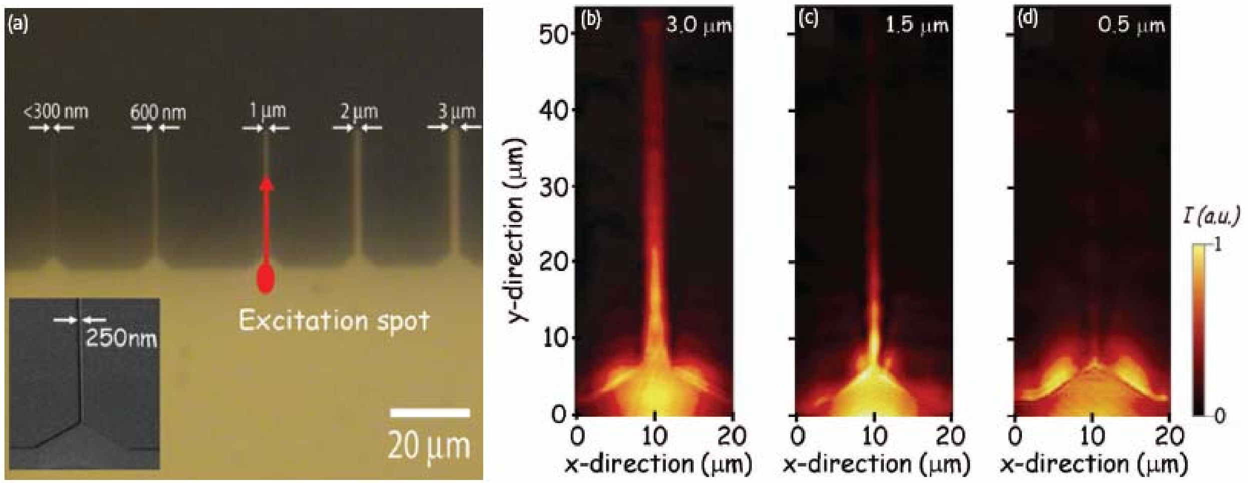

Fig. 3 (a) Optical microscopy image of a SiO_2 substrate with an array of Au stripes attached to a large launchpad generated by electron beam lithography. The red arrow illustrates the launching of an SPP into a 1 µm wide stripe. (b, c, and d) PSTM images of SPPs excited at λ = 780 nm and propagating along 3.0 µm, 1.5 µm, and 0.5 µm wide Au stripes, respectively. (Parts b,c, and d reprinted with permission from[23]. © American Physical Society.)

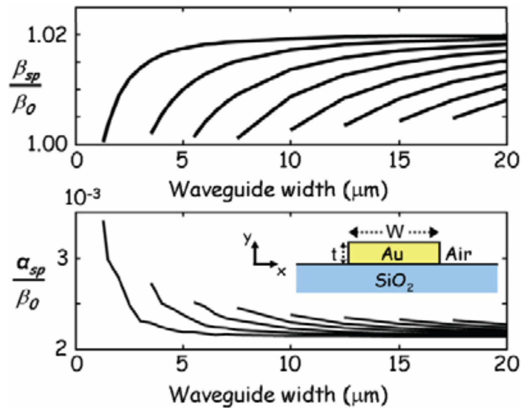

Fig. 5 Calculated complex propagation constants ($\beta_{sp} + i\,\alpha_{sp}$) for the eight lowest order leaky, quasi-TM SPP modes of varying width Au stripe waveguides. For these calculations, the Au stripe thickness was t = 55 nm and the free space excitation wavelength was λ = 800 nm. The magnitudes of β_{sp} and α_{sp} were normalized to the real part of the free space propagation constant β_0. The inset shows the simulation geometry and the coordinate frame. (Reprinted with permission from[21]. © 2005 American Physical Society.)

Propagation distance decreases with decreasing strip width !

materialstoday JULY-AUGUST 2006 | VOLUME 9 | NUMBER 7-8

Bound and leaky SPP modes

Au strip on SiO_2 substrate:

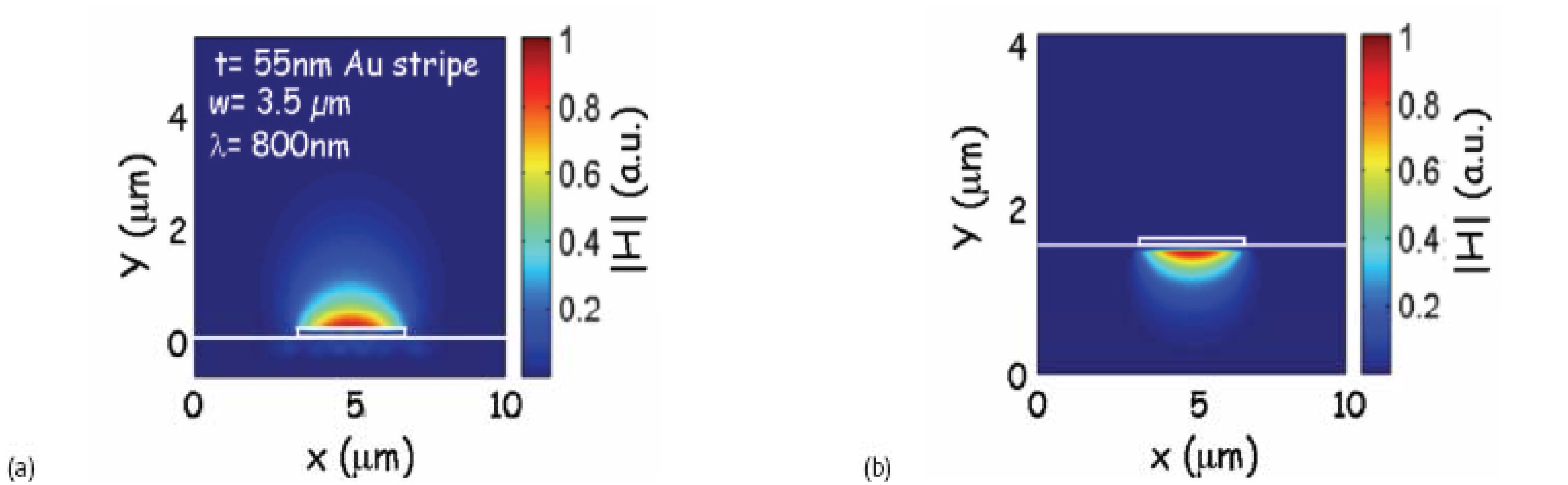

Fig. 4 Simulated SPP mode profiles for a 55 nm thick and 3.5 μm wide Au stripe on a SiO_2 glass substrate. It shows the fundamental leaky (left) and bound (right) SPP modes propagating at the top air/metal and bottom glass/metal interfaces, respectively. Both modes can be employed simultaneously for information transport. (Reprinted with permission from[21]. © 2005 American Physical Society.)

JULY-AUGUST 2006 | VOLUME 9 | NUMBER 7-8 materialstoday

SPP modes can occur on the top (Au-air interface -> leaky mode)) and the bottom (Au- SiO_2 Interface -> bound mode)

Both modes can simultaneously carrying information without interacting

SPPs at IMI/MIM interfaces

Comparison of two different waveguide configurations

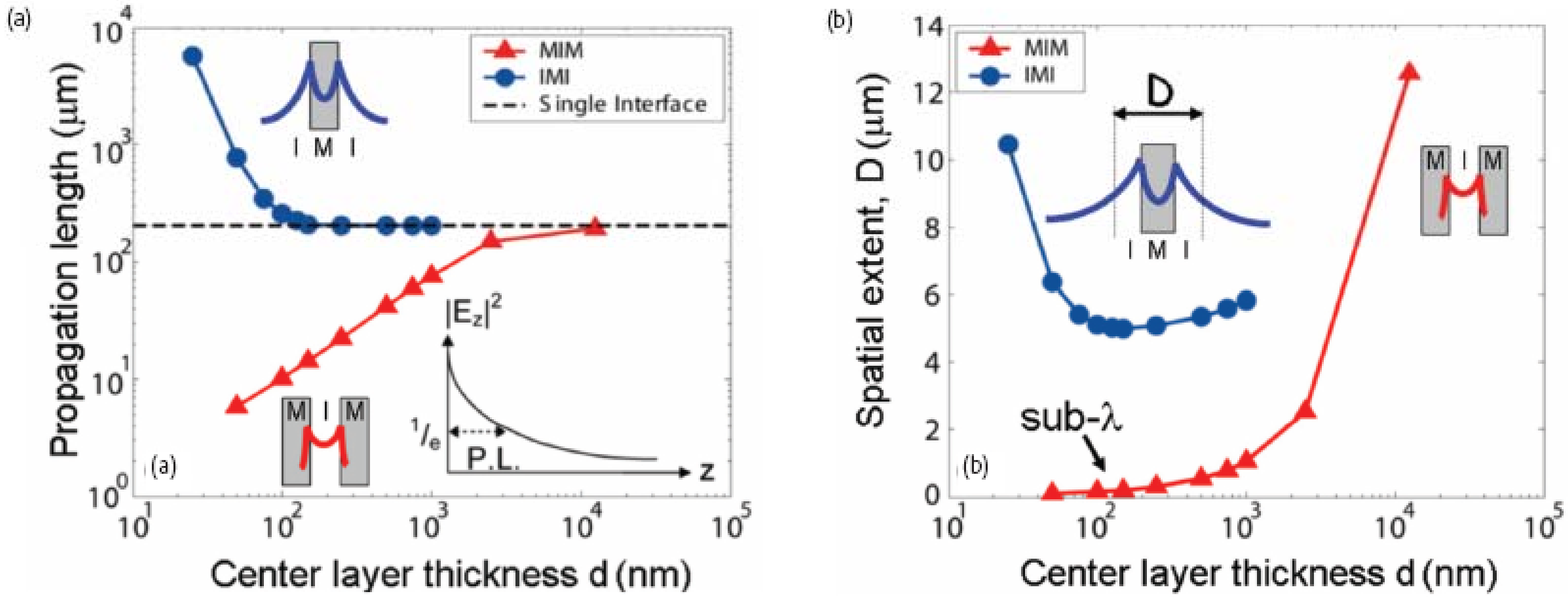

Fig. 6 Plot of (a) SPP propagation length and (b) spatial extent of the SPP modes as a function of the center-layer thickness for MIM and IMI plasmonic waveguides. The insets illustrate plotted terms. The reflection pole method was used for λ = 1.55 µm with Au as the metal and air as the insulator. (Reprinted with permission from[19]. © 2004 The Optical Society of America.)

There is a trade-off between confinement and propagation distance of SPPs !

Absorption of metal nanoparticles

Lycurgus Cup

LYCURGUS CUP, a Roman goblet dating from the fourth century A.D., changes color because of the plasmonic excitation of metallic particles within the glass matrix. When a light source is placed inside the normally greenish goblet, it looks red.

in reflection

in transmission

a)

b)

Au NP

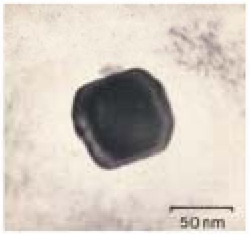

Plasmon-resonance absorption of colliodal Au NPs

c)

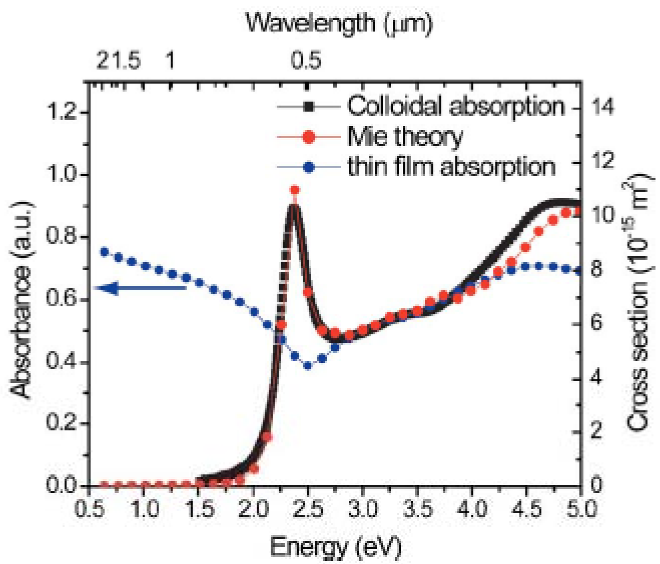

JOURNAL OF APPLIED PHYSICS 98, 011101 (2005)

Strength of the free-carrier absorption is pulled into the particle plasmon resonance.

Absorption of metal nanoparticles

Enhanced local electric field in metallic NPs

Dependence of plasmon resonance induced absorption from size and shape of colloidal Ag NPs

ABB. 1 | NAHFELD UM NANOPARTIKEL

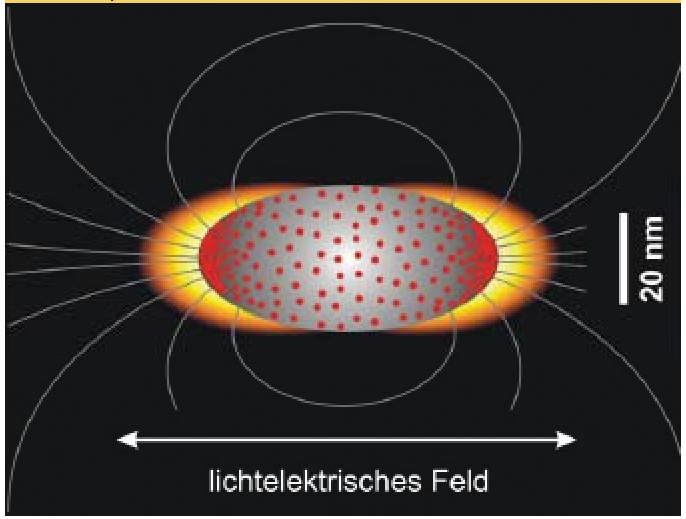

Metallisches Nanopartikel im lichtelektrischen Feld. Die roten Punkte sind die oszillierenden Elektronen, der gelbliche „Schein“ um das Partikel zeichnet die Intensität des optischen Nahfeldes nach (hell: hohe Intensität).

ABB. 2 | FORM UND LICHTABSORPTION

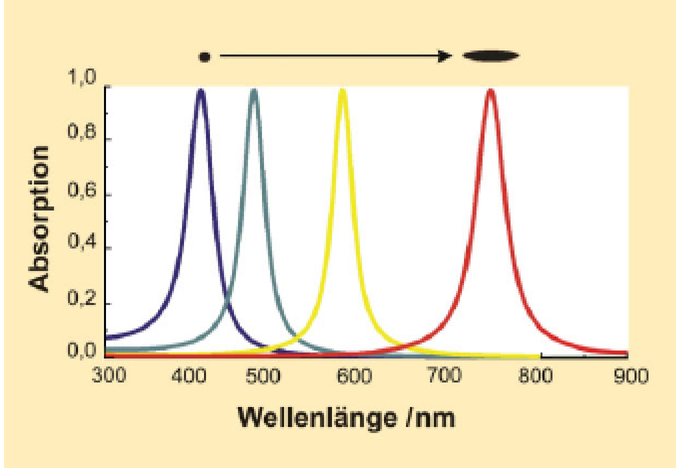

Lichtabsorptionsspektren metallischer Nanopartikel (Silber) als Folge der plasmonischen Resonanz. Wie oben angedeutet, variiert die Form der Partikel von kugelförmig (links) bis gestreckt (rechts).

www.phiuz.de 5/2006 (37) | Phys. Unserer Zeit | 221

⇨ Deviation from spherical NP geometry can lead to additional plasmon resonance frequencies

Absorption of metal nanoparticles

From spherical NPs to complex structures

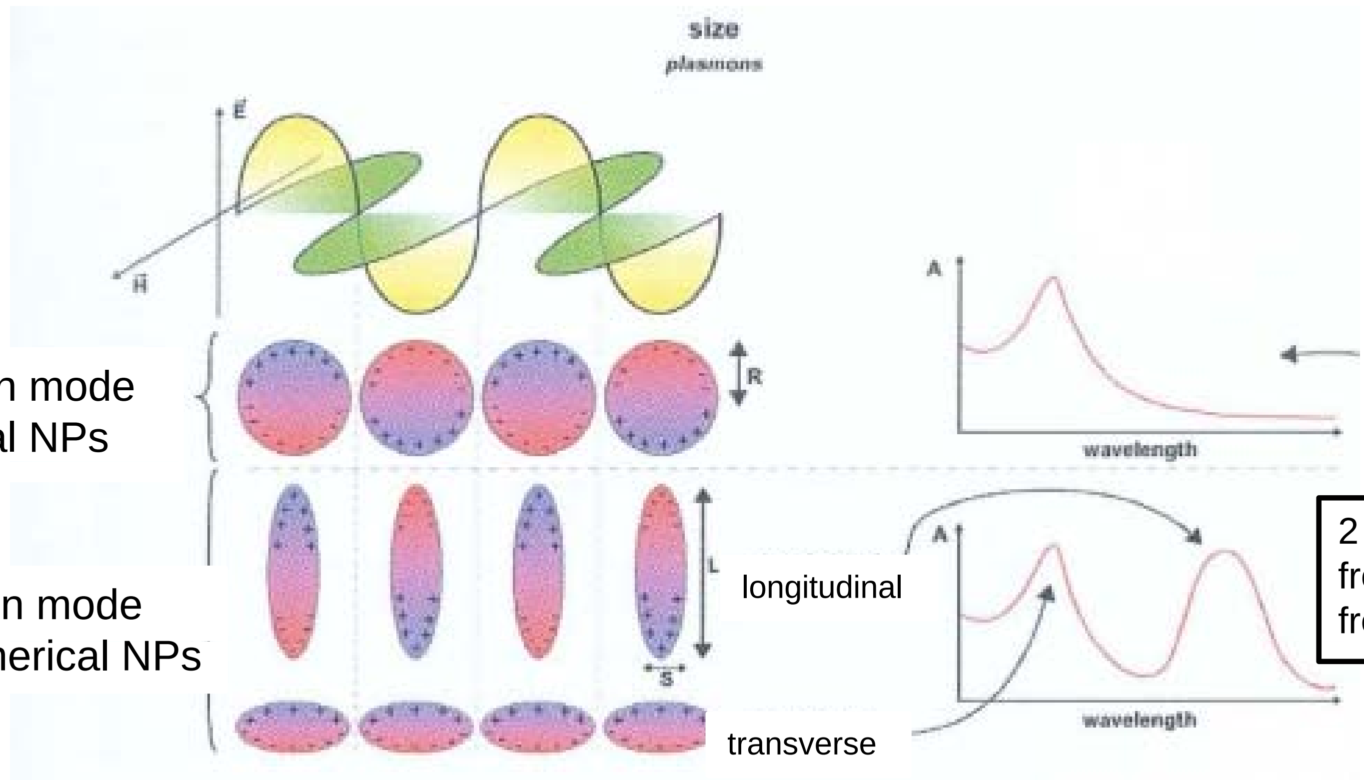

1 excitation mode in spherical NPs

2 excitation mode in non-spherical NPs

longitudinal

transverse

1 peak

2 peaks derive from 2 resonance frequencies

Absorption of metal nanoparticles

From spherical NPs to complex structures

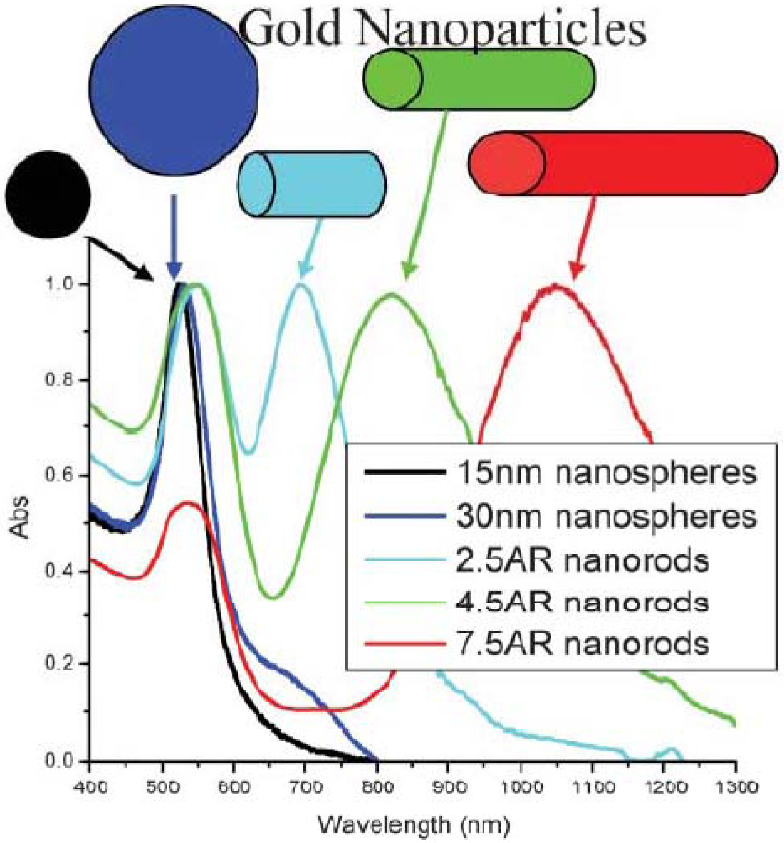

Light scattering at Au nanoparticles

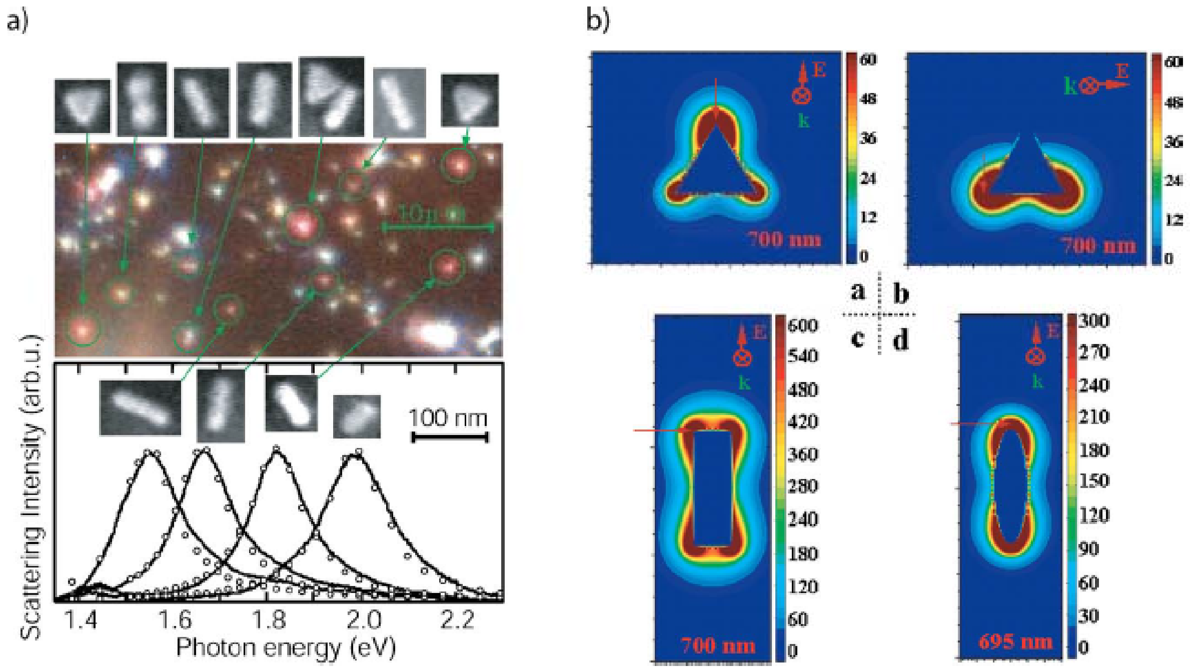

FIG. 2. (Color online) (a) Dark-field microcopy image (top) and light-scattering spectra (bottom) of Au nanocrystals of different shapes (adapted from Ref. 17). The measured spectra (black curves) show good agreement with predictions from a simple analytical extension of quasi-static Mie theory (open circles). (b) Electric near-field profile of the lowest-order modes of Ag nanoprisms calculated using the discrete dipole approximation formalism (adapted from Ref. 54).

JOURNAL OF APPLIED PHYSICS **98**, 011101 (2005)

Light scattering at metallic NPs

- conduction electrons confined in small metal particle
- incident plane wave: electrons move coherently, in phase
- charge-buildup at particle surface with frequency of wave
- leads to particle-specific restoring force

-> particle dipole plasmon frequence

-> redshifted with increasing particle size

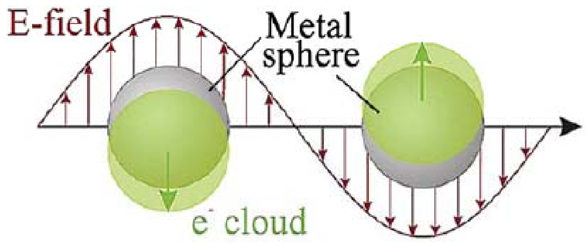

Plasmonics (2006) 1: 5–33
DOI 10.1007/s11468-005-9002-3

Polarizability α of a sperical NP with radis a << λ:

$$\alpha = 4\pi a^3 \frac{\varepsilon - \varepsilon_m}{\varepsilon + 2\varepsilon_m},$$

Polarizability α for ellipsoidal NPs with axes a,b,c :

$$\alpha = \frac{4}{3}\pi abc \frac{\varepsilon - \varepsilon_m}{\varepsilon_m + L_i(\varepsilon - \varepsilon_m)}, \quad \sum L_i = 1.$$

Applications for Plasmonics

New device types for optoelectronics

Simulations can be applied

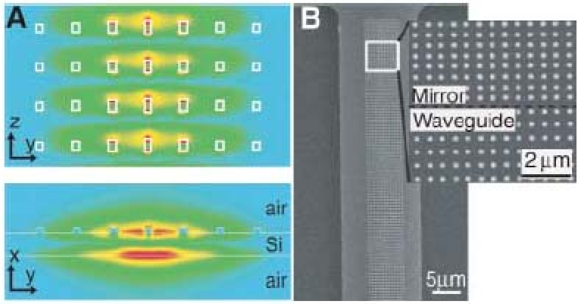

Fig. 1. (**A**) FDTD simulations show the electric field produced within the plasmon waveguide structure. (**B**) A plasmon waveguide consists of nanoscale gold dots on a silicon-on-insulator surface. [Adapted from (*9*)]

Predictions for device development

Plasmonics: Merging Photonics and Electronics at Nanoscale Dimensions
Ekmel Ozbay, *et al.*
Science **311**, 189 (2006);
DOI: 10.1126/science.1114849

Combination of plasmonic waveguide and plasmonic condensor for focussing

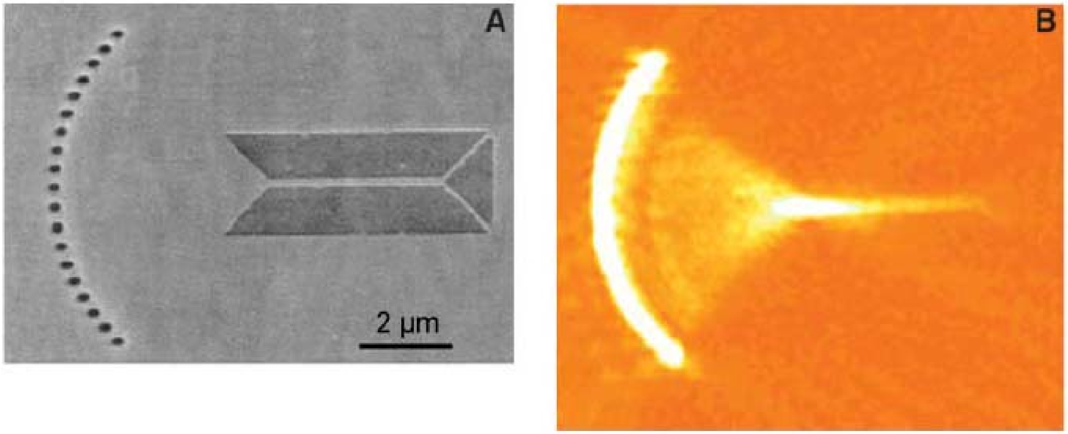

Fig. 2. (**A**) SEM image of a nanodot focusing array coupled to a 250-nm-wide Ag strip guide. (**B**) NSOM image of the SP intensity showing subwavelength focusing. [Adapted from (*15*)]

Applications for Plasmonics

Integration into chips to speed up data processing

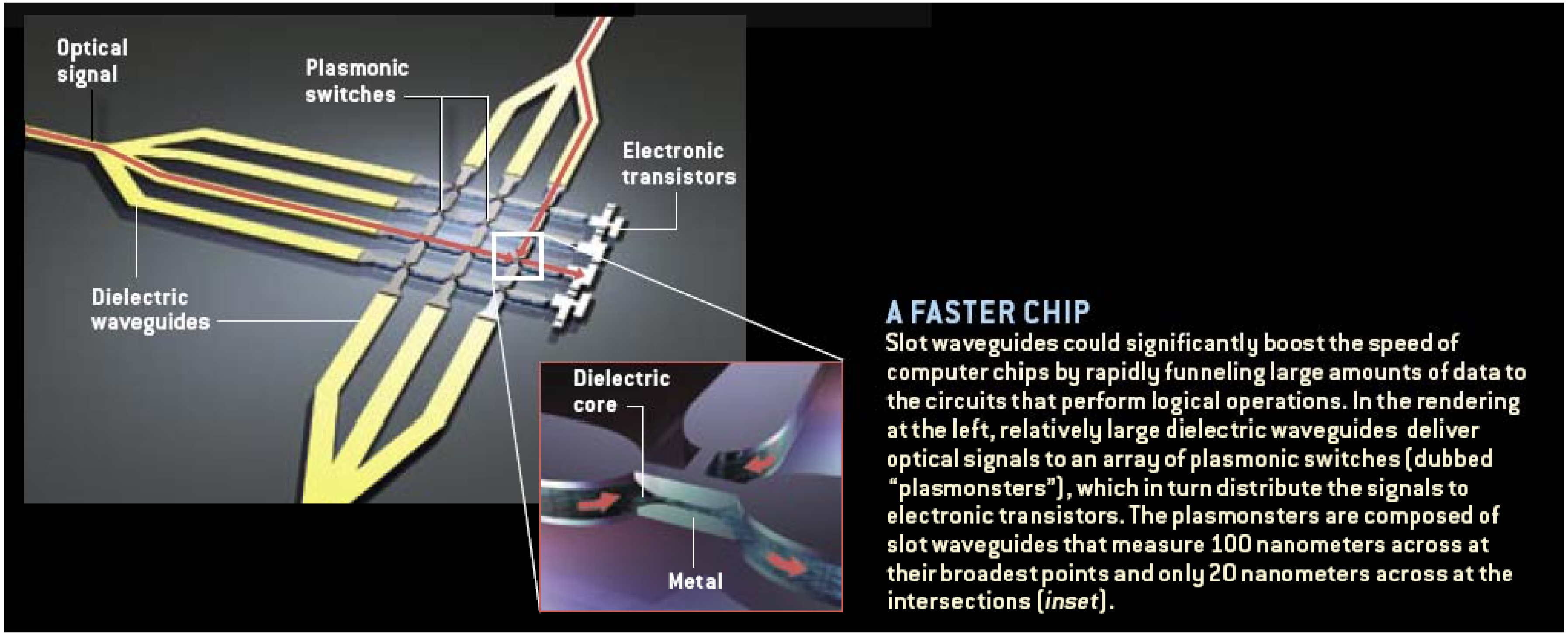

Applications for Plasmonics

Generation and manipulation of electromagnetic radiation

⇨

Plasmonics: Merging Photonics and Electronics at Nanoscale Dimensions
Ekmel Ozbay, *et al.*
Science **311**, 189 (2006);
DOI: 10.1126/science.1114849

Subwavelength aperture

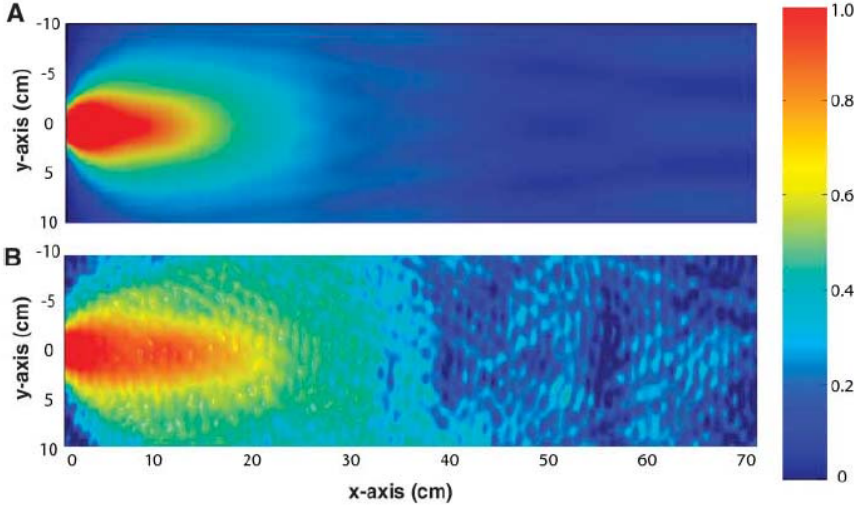

Fig. 3. Calculated (**A**) and measured (**B**) electric field distribution from a subwavelength circular annular aperture with a grating at the resonance frequency. The measured electric field intensity is confined to a narrow spatial region and propagates without diffracting into a wide angular region, which is in good agreement with the simulations.

Nanolithography

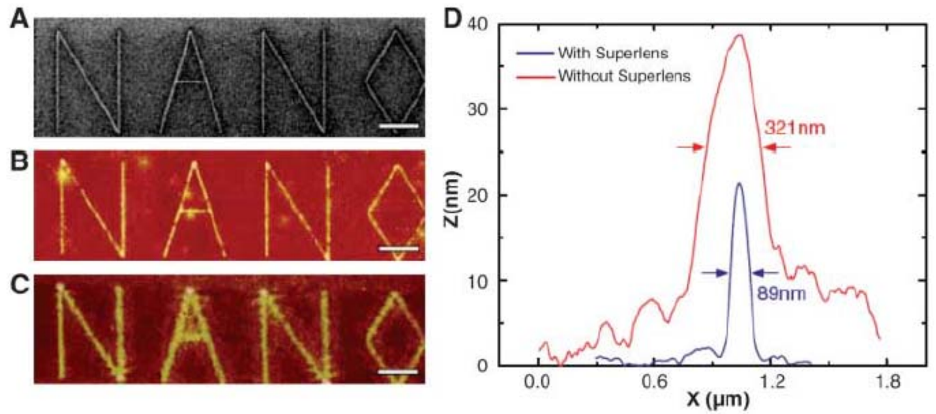

Fig. 4. The images of an arbitrary object obtained by different methods. (**A**) FIB image of the object. (**B**) The image obtained on photoresist with a silver superlens. (**C**) The image obtained on photoresist with conventional lithography. (**D**) Comparison of both methods. [Adapted from (*40*)]

Applications for Plasmonics

Lithography

Figure 42. AFM image of a pattern with 90-nm features with a period of 170 nm prepared by surface plasmon lithography (left) and 3D image of this structure (right). From [131].

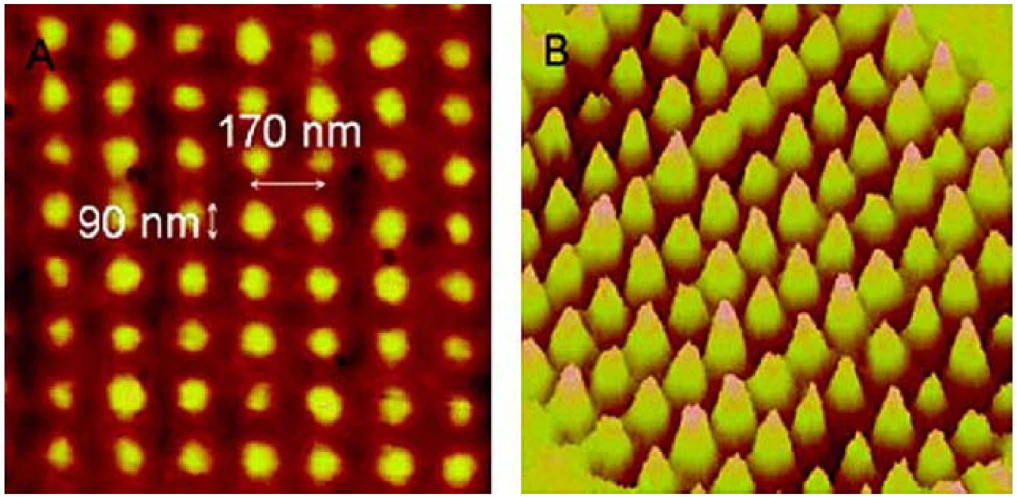

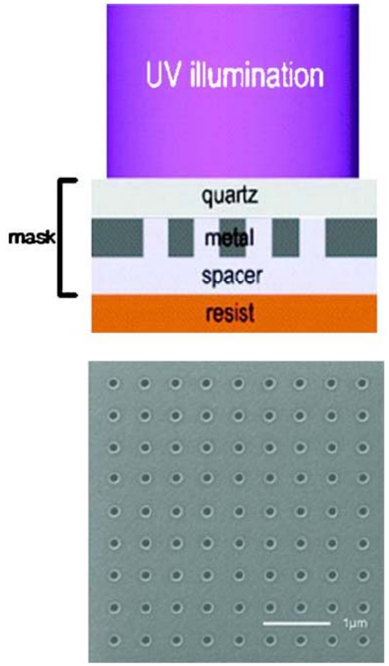

Figure 41. Top, schematic of the surface plasmon optical lithography. Bottom, focused ion beam image of a hole array mask with hole size of 160 nm and period of 500 nm. From [131].

Plasmonics (2006) 1: 5–33
DOI 10.1007/s11468-005-9002-3

Applications for Plasmonics

Coupling and polarization effects

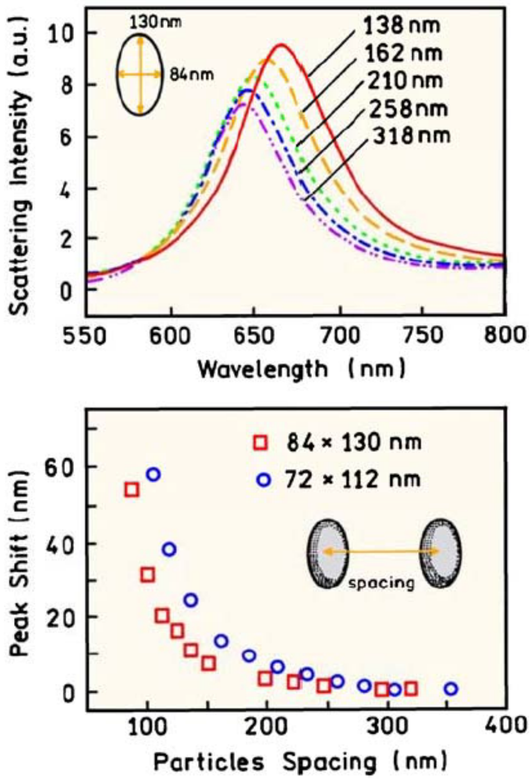

Figure 16. Scattering spectra and peak scattering wavelengths calculated for two elliptical disks at varying center-to-center distances. Top, the numbers on the right indicate the particle center-to-center distances. Revised from [71].

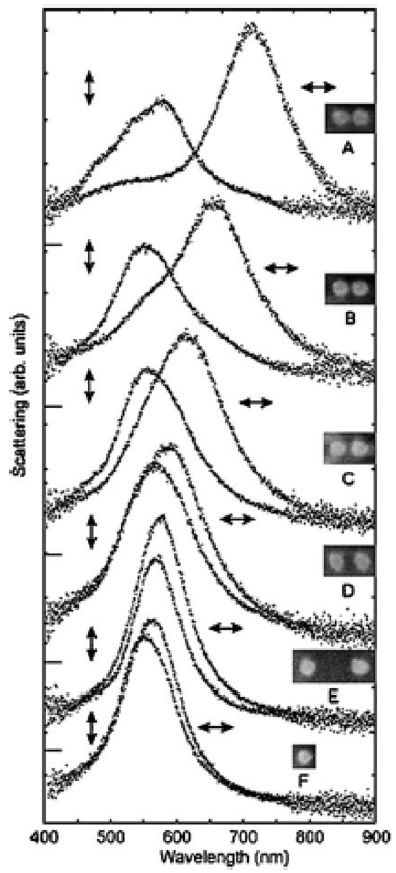

Figure 17. Dark-field scattering spectra and scanning electron micrography of isolated disk-shaped particle pairs. The arrows indicate the polarization of the incident light. The gaps between the particles are approximately 10, 15, 25, 50, and 250 nm, for A through E. F is an isolated particle. The disks are about 95 nm in diameter and 25 nm high. From [72].

Plasmonics (2006) 1: 5–33
DOI 10.1007/s11468-005-9002-3

⇨ **Sub-wavelength Distance measurements**

Applications for Plasmonics

Enhanced flourescence in the presence of a background

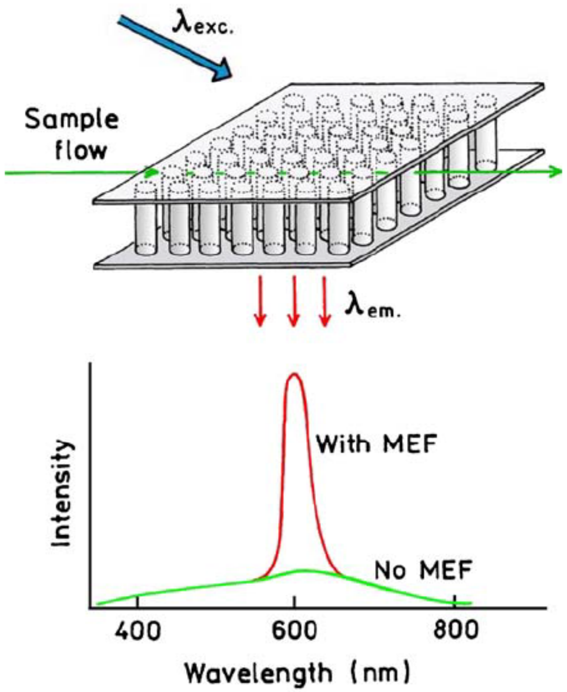

Figure 22. Schematic of wavelength-selective enhanced fluorescence in the presence of background. Top, represents an array of metal nanowires spanning the top and bottom of a flow cell.

Chain of metal nanoparticles

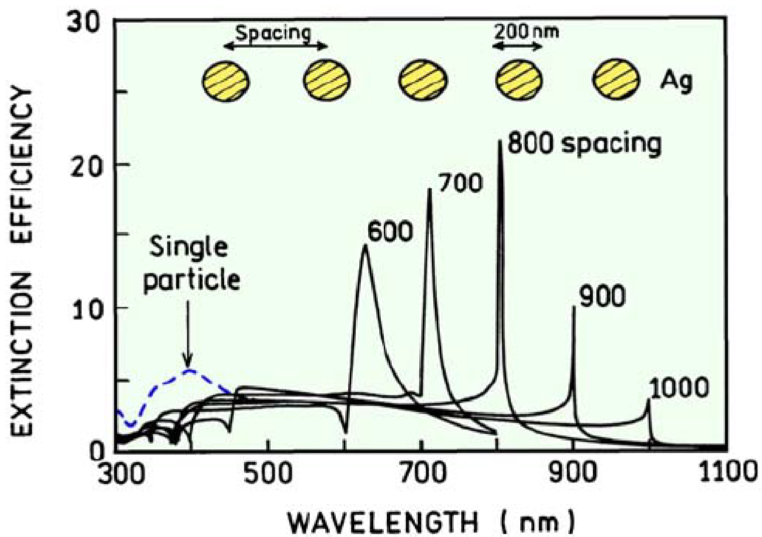

Figure 23. Extinction spectra for a one-dimensional chain of silver nanoparticles. Revised from [82].

Plasmonics (2006) 1: 5–33
DOI 10.1007/s11468-005-9002-3

Applications for Plasmonics

Core-shell particles as nanoprobes

Increased fluorescence intensity:
-> waveenth is adjustable

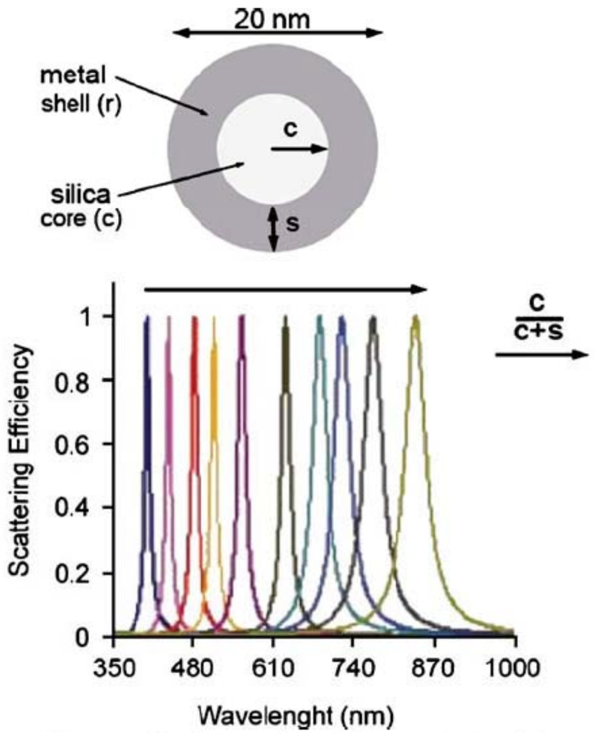

Figure 28. Normalized scattering efficiency calculated for metal nanoshells on silica cores. Revised from [96].

FIB structure in Ag film
-> sharp light transmission

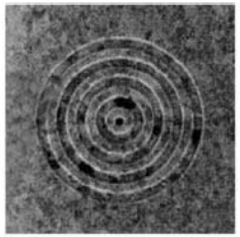

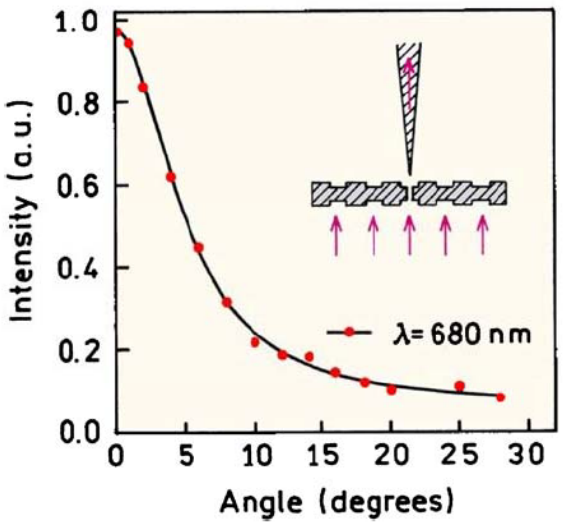

Figure 40. Top, focused ion beam micrograph of a silver film, 300 nm thick, 350-nm hole diameter, 500-nm periodicity with 60-nm-deep groves. Bottom, angular distribution of transmitted light at 660 nm. Revised from [127].

Plasmonics (2006) 1: 5–33
DOI 10.1007/s11468-005-9002-3

(without structure:-> full scattering)

Applications for Plasmonics

Cancer therapy utilizing core-shell NPs

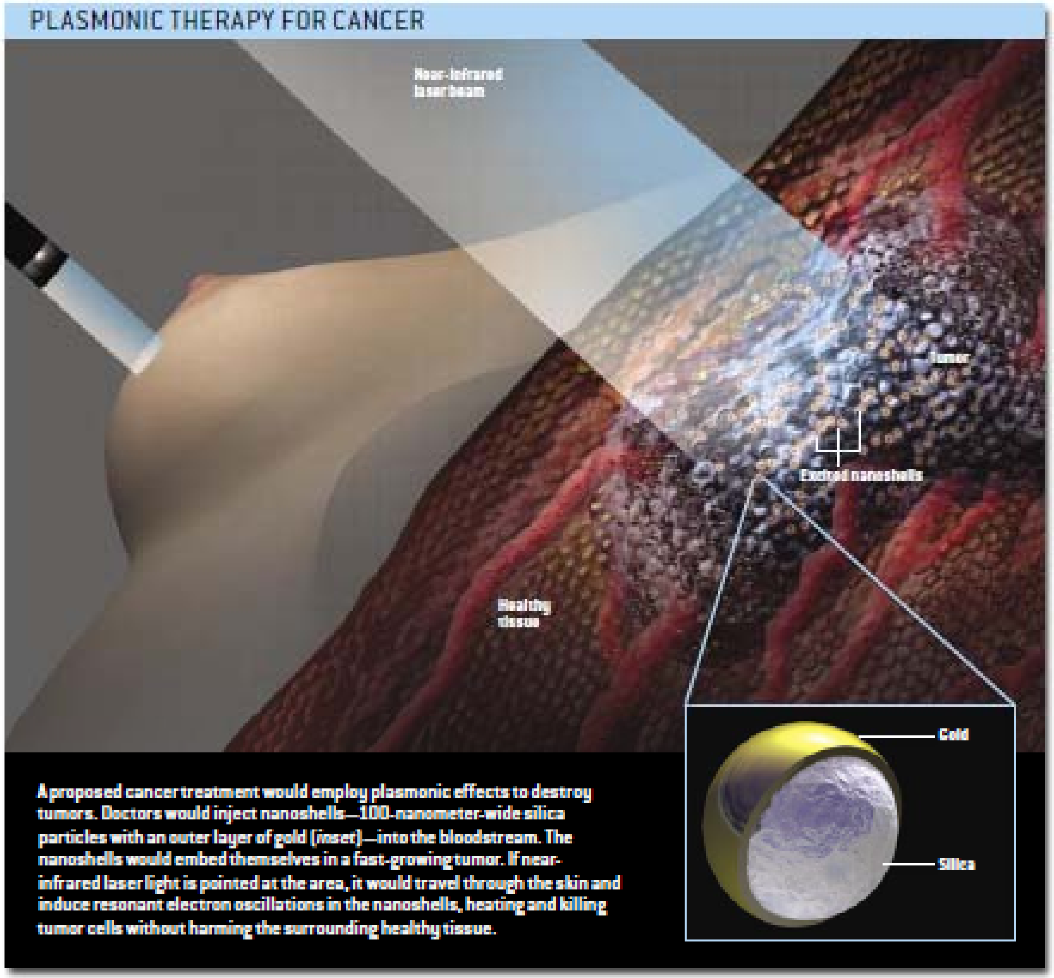

Applications for Plasmonics

Proposed subwavelength plasmonic microscope

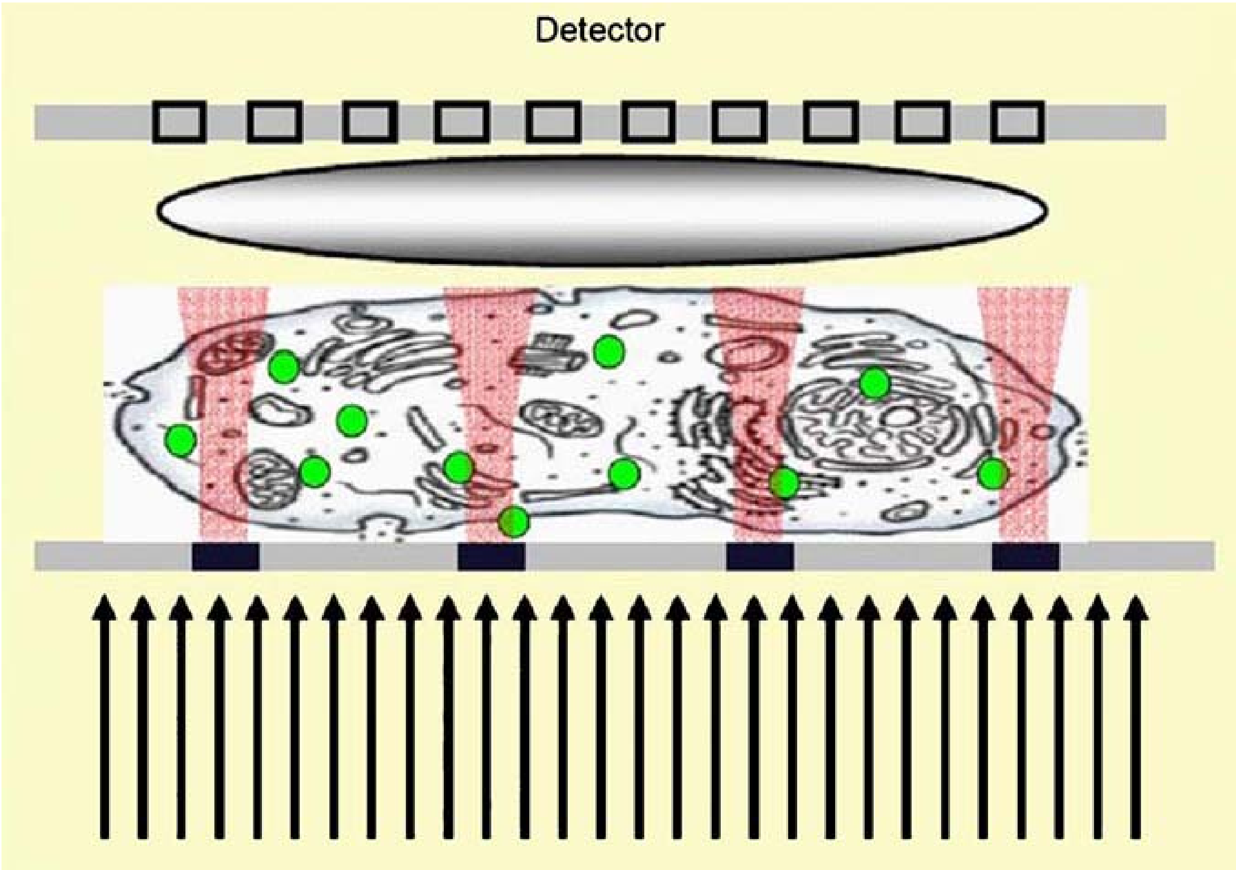

Detection of fluorescence

Fluorophor labeled sample

Nanohole array

-> taking of multiple images by moving the nanohole array and reconstruct them

Spatial resolution down to 25 nm should be achievable !

Plasmonics (2006) 1: 5–33
DOI 10.1007/s11468-005-9002-3